Polyphyllin II inhibits thyroid cancer progression by targeting HRH1 and suppressing Wnt/β-catenin signaling

JIANWEI SUN[1], HAIFENG LIANG[2], YAN ZHANG[2], DING DING[1], QIAN XIANG[3], MENGYANG ZHENG[1] and PENGYUE ZHANG[4]

[1]Department of Ultrasound, The Fifth Affiliated Hospital of Kunming Medical University, Gejiu, Yunnan 661000, P.R. China; [2]Department of Oncology, The Fifth Affiliated Hospital of Kunming Medical University, Gejiu, Yunnan 661000, P.R. China; [3]Department of Endocrinology, The Fifth Affiliated Hospital of Kunming Medical University, Gejiu, Yunnan 661000, P.R. China; [4]Key Laboratory of Acupuncture and Massage for Treatment of Encephalopathy, College of Acupuncture, Tuina and Rehabilitation, Yunnan University of Chinese Medicine, Kunming, Yunnan 650500, P.R. China

Received January 30, 2026; Accepted June 19, 2026

DOI: 10.3892/or.2026.9168

Abstract. Polyphyllin II, a natural steroidal saponin extracted from *Paris polyphylla*, exhibits potent antitumor activity in thyroid cancer. In the present study, bioinformatics analysis, molecular docking, Drug Affinity Responsive Target Stability assay, Cell Counting Kit-8 assay, flow cytometry, Transwell assay, wound-healing assay, reverse transcription-quantitative PCR, western blotting and xenograft experiments were performed to investigate the antitumor effects and molecular mechanism of polyphyllin II in thyroid cancer. Polyphyllin II significantly inhibited cell proliferation, migration and invasion, while inducing apoptosis more prominently in TPC-1 cells and causing cell cycle arrest in both TPC-1 and 8305C cells. By using integrated bioinformatics screening and experimental validation, histamine receptor H1 (HRH1) was identified as a key oncogenic target that is highly expressed in thyroid cancer and contributes to malignant progression. With regard to its mechanism of action, polyphyllin II suppressed HRH1-mediated activation of the Wnt/β-catenin signaling pathway, reduced β-catenin nuclear accumulation and downregulated the expression levels of downstream pathway-related genes. Collectively, these findings demonstrate that polyphyllin II attenuates thyroid cancer progression by targeting HRH1 and blocking Wnt/β-catenin signaling, highlighting its potential as a promising candidate for targeted therapy.

Correspondence to: Dr Pengyue Zhang, Key Laboratory of Acupuncture and Massage for Treatment of Encephalopathy, College of Acupuncture, Tuina and Rehabilitation, Yunnan University of Chinese Medicine, 1076 Yuhua Road, Chenggong, Kunming, Yunnan 650500, P.R. China
E-mail: zhangpengyue@ynutcm.edu.cn

Abbreviations: TC, Thyroid cancer; DTC, differentiated thyroid cancer; ATC, anaplastic thyroid carcinoma; HRH1, histamine receptor H1; Wnt/β-catenin, Wnt/β-catenin signaling pathway; MMP7, matrix metalloproteinase 7; WNT7A, Wingless-type MMTV integration site family member 7A; CCK-8, Cell Counting Kit-8; PBS, phosphate-buffered saline; DMSO, dimethyl sulfoxide; RT-qPCR, reverse transcription quantitative PCR; WB, western blotting; FITC, fluorescein isothiocyanate; GAPDH, glyceraldehyde-3-phosphate dehydrogenase

Key words: polyphyllin II, thyroid cancer, histamine receptor H1, Wnt/β-catenin signaling pathway

Introduction

Thyroid cancer is the most common malignancy of the endocrine system and its global incidence has steadily increased over the past decade (1). The majority of the thyroid cancers arise from the follicular epithelium and are classified as papillary thyroid carcinoma or follicular thyroid carcinoma, collectively classified as differentiated thyroid carcinoma (DTC) (2). DTC accounts for >90% of all thyroid cancer cases, generally indicating a favorable prognosis under standard treatment (3). However, 20-30% of patients with DTC experience recurrence and ~5% develop distant metastasis, negatively affecting long-term survival (4). Medullary thyroid carcinoma, poorly differentiated thyroid carcinoma and anaplastic thyroid carcinoma (ATC) represent more aggressive subtypes, with ATC accounting for ~40% of TC-related deaths despite its low incidence (5). Due to limited responsiveness to radioactive iodine therapy in advanced disease, notably ATC and radioiodine-refractory DTC, novel therapeutic approaches are urgently required to improve clinical outcomes (6).

In current endocrine and surgical oncology practice, accurate risk stratification of thyroid nodules and thyroid cancer remains challenging, particularly for indeterminate thyroid nodules and aggressive or treatment-resistant tumors. Although cytology, imaging and molecular testing have improved clinical decision-making, reliable biomarkers for predicting malignancy, progression and prognosis are still needed. Studies have also suggested that systemic inflammatory markers, such as neutrophil-to-lymphocyte ratio, lymphocyte-to-monocyte ratio and platelet-to-lymphocyte

ratio, may be associated with thyroid cancer behavior and clinical outcomes (7,8). These findings indicate that thyroid cancer progression is closely related not only to intrinsic oncogenic signaling but also to inflammatory and immune-related regulation. Therefore, identifying novel therapeutic targets and effective molecular interventions remains important for improving thyroid cancer management.

Polyphyllin II is a steroidal saponin purified from *Paris polyphylla*, a medicinal herb with broad anticancer activity (9). Previous studies have reported that polyphyllin II suppresses tumor progression by inducing apoptosis, inhibiting cell motility and modulating autophagy in cancer types such as colorectal carcinoma and osteosarcoma (10-12). However, its role in thyroid cancer remains poorly understood and the molecular targets responsible for its anticancer effects have not been fully elucidated. Therefore, the investigation of the pharmacological mechanism of polyphyllin II may provide a novel therapeutic avenue for thyroid cancer intervention.

In the present study, bioinformatics screening and functional assays were integrated to identify key genes affected by polyphyllin II in thyroid cancer cells. It was demonstrated that polyphyllin II suppressed malignant behaviors by targeting histamine receptor H1 (HRH1) and consequently modulating the Wnt/β-catenin signaling pathway.

Materials and methods

Cell culture and treatments. Human thyroid cancer cell lines TPC-1 and 8305C were purchased from Cell Resource Center, Shanghai Institute for Biological Sciences, Chinese Academy of Sciences (https://www.cellbank.org.cn/index.php). The normal human thyroid epithelial cell line Nthy-ori 3-1 was used as a non-malignant control, and was purchased from Procell Life Science & Technology Co., Ltd. TPC-1 is a papillary thyroid carcinoma cell line and represents differentiated thyroid cancer, whereas 8305C is an anaplastic thyroid carcinoma cell line and represents a highly aggressive and poorly differentiated thyroid cancer subtype. These two cell lines were selected to evaluate the antitumor effect of polyphyllin II in thyroid cancer models with different histological origins and malignant potential.

TPC-1, 8305C, and Nthy-ori 3-1 cells were cultured in Dulbecco's Modified Eagle Medium (DMEM; Wisent Biotechnology; cat. no. 319-005-CL) supplemented with 10% fetal bovine serum (Wisent Biotechnology; cat. no. 086-150), 100 U/ml penicillin (Wisent Biotechnology; cat. no. 450-201-EL), and 100 μg/ml streptomycin (Wisent Biotechnology; cat. no. 450-201-EL). Cells were maintained in a humidified incubator at 37˚C with 5% CO_2.

Polyphyllin II was dissolved in dimethyl sulfoxide (DMSO) to prepare a stock solution and diluted to the desired concentrations with complete culture medium immediately before use. Initially, it was determined whether there was cytotoxicity based on the half-maximal inhibitory concentration (IC_{50}). Finally, 5 μg/ml was selected for the subsequent cell experiments.

Lentiviral transduction. Lentiviral vectors used for HRH1 knockdown and overexpression were constructed by GeneChem Co., Ltd. For HRH1 silencing, a short interfering (sh)RNA sequence targeting human HRH1 was designed as follows: sh-HRH1, 5'-GCTCTGGTTCTATGCCAAGAT-3'. A non-targeting shRNA sequence, 5'-TTCTCCGAACGTGTC ACGT-3', was used as the negative control (sh-NC). For HRH1 overexpression, the full-length human HRH1 coding sequence was cloned into a lentiviral overexpression vector to generate overexpression (OE)-HRH1, while the corresponding empty vector was used as the NC.

Lentiviral particles were produced using a third-generation lentiviral packaging system. Briefly, 293T cells were obtained from the Cell Resource Center, Shanghai Institute for Biological Sciences, Chinese Academy of Sciences and cultured in DMEM supplemented with 10% FBS (Procell Life Science & Technology Co., Ltd.; cat. no. PM150210B). When the cells reached 70-80% confluence, they were co-transfected with the lentiviral expression plasmid, packaging plasmids and envelope plasmid at a mass ratio of 4:3:2:1 using Lipofectamine® 3000 reagent (Invitrogen; Thermo Fisher Scientific, Inc.) according to the manufacturer's instructions. The total amount of plasmid DNA used for each 10-cm dish was 20 μg. The culture supernatant containing lentiviral particles was collected at 48 and 72 h after transfection, centrifuged at 1,000 x g for 10 min at 4˚C to remove cell debris and filtered through a 0.45-μm filter. TPC-1 and 8305C cells were transduced with the indicated lentiviral particles in the presence of 5 μg/ml polybrene (Shanghai Yeasen Biotechnology Co., Ltd.; cat. no. 40804ES76). The multiplicity of infection was 20 for TPC-1 cells and 30 for 8305C cells. Following 48-72 h of transduction, stable cells were selected using 2 μg/ml puromycin (Shanghai Yeasen Biotechnology Co., Ltd.; cat. no. 727136ES01) for 7 days and maintained in medium containing 1 μg/ml puromycin. The efficiency of HRH1 knockdown or overexpression was verified by reverse transcription-quantitative PCR and western blotting before subsequent experiments.

Data collection and analysis. The GSE197443 dataset was obtained from the Gene Expression Omnibus database (https://www.ncbi.nlm.nih.gov/gds) and differentially expressed gene analysis was performed using the GEO2R online tool (https://www.ncbi.nlm.nih.gov/geo/geo2r/). The resulting data were imported into TBtools II software (version 2.096; https://github.com/CJ-Chen/TBtools) to create volcano plots. The simplified molecular input line notation information of polyphyllin II was obtained from the PubChem database (https://pubchem.ncbi.nlm.nih.gov/) and imported into the SwissTarget database (http://www.swisstargetprediction.ch/) to predict its potential target genes. The intersection of upregulated differentially expressed genes and polyphyllin II target genes was visualized using the Venn diagram plugin of TBtools II software. The RNA sequencing data of The Cancer Genome Atlas (TCGA)-thyroid cancer (THCA) project were downloaded and processed from the TCGA database (https://portal.gdc.cancer.gov). Gene expression profiles were analyzed using the stats package (version 4.3.2, https://www.r-project.org/) and car package(version 3.1-2, https://cran.r-project.org/package=car), while single-gene differential association analysis was conducted using the DESeq2 package(version 1.52.0, https://bioconductor.org/packages/DESeq2/). Enrichment analysis was employed

to identify Gene Ontology (GO) and Kyoto Encyclopedia of Genes and Genomes (KEGG) functional annotations. GO analysis and KEGG pathway analysis were performed using the clusterProfiler package (version 4.20.0, https://bioconductor.org/packages/clusterProfiler/) with a significance threshold of $q<0.05$.

Cell proliferation assay [Cell Counting Kit-8 (CCK-8)]. TPC-1 and 8305C cells were seeded into 96-well plates at a density of $5x10^4$ cells/well. Following cell adherence, cells were treated with 0, 1, 5, 10 and 20 μg/ml polyphyllin II or vehicle control for 24 h at 37˚C. Following incubation, 10 μl CCK-8 reagent (Beyotime Biotechnology; cat. no. C0037) was added to each well and incubated for 2 h at 37˚C. The absorbance was measured at 450 nm using a microplate reader to assess proliferation activity.

Apoptosis analysis by flow cytometry. TPC-1 and 8305C cells were seeded into six-well plates and treated with 5 μg/ml polyphyllin II or vehicle control for 24 h at 37˚C. After treatment, cells were harvested, washed with cold phosphate-buffered saline (PBS) and resuspended in binding buffer. The cells were then stained with Annexin V- fluorescein isothiocyanate (FITC) and propidium iodide according to the manufacturer's instructions. After incubation for 15 min at room temperature in the dark, apoptotic cells were detected using a flow cytometer (LongCyte; Beijing Challen Biotechnology Co., Ltd.). Flow cytometry data were acquired and analyzed using ModelFlower software (version 2.0, Beijing Challen Biotechnology Co., Ltd.). The apoptosis rate was calculated as the percentage of early and late apoptotic cells. Each experiment was independently repeated at least three times.

Cell cycle analysis by flow cytometry. TPC-1 and 8305C cells were seeded into six-well plates and treated with 5 μg/ml polyphyllin II or vehicle control for 24 h at 37˚C. After treatment, cells were harvested, washed twice with cold PBS, and fixed with 70% ethanol at 4˚C overnight. The fixed cells were then washed with PBS and incubated with propidium iodide/RNase staining solution for 30 min at room temperature in the dark according to the manufacturer's instructions. After incubation for 30 min at room temperature in the dark, cell cycle distribution was analyzed using a flow cytometer (LongCyte; Beijing Challen Biotechnology Co., Ltd.). Flow cytometry data were acquired and analyzed using ModelFlower software (version 2.0, Beijing Challen Biotechnology Co., Ltd.). The percentages of cells in the G_0/G_1, S, and G_2/M phases were calculated. Each experiment was independently repeated at least three times.

Transwell invasion assay. The upper chambers of Transwell inserts (MilliporeSigma; cat. no. PI8P01250) were precoated with Matrigel matrix (MilliporeSigma; cat. no. CLS356237) and air-dried at 37˚C for 2 h to allow gel formation. TPC-1 and 8305C cells were pretreated with 5 μg/ml polyphyllin II or vehicle control for 24 h at 37˚C before being seeded into the upper chambers. Cells suspended in serum-free medium were added to the upper chambers at a density of $5x10^5$ cells/well, while complete medium containing 10% fetal bovine serum (Wisent Biotechnology; cat. no. 086-150) was added to the lower chambers as a chemoattractant. Following incubation for 24 h at 37˚C, the cells that invaded through the membrane were fixed with 2.5% paraformaldehyde (Coolaber; cat. no. SL1770) for 20 min at room temperature and stained with 0.1% crystal violet (Beyotime Biotechnology; cat. no. C0121) for 20 min at room temperature. The number of invaded cells was imaged and quantified under a microscope.

Wound healing migration assay. The cells were seeded into six-well plates at a density of $2x10^5$ cells/well and grown to 100% confluence. A sterile 200 μl pipette tip was used to scratch straight lines on the monolayer surface. Detached cells were washed away with PBS and the remaining cells were incubated with serum-free medium containing 5 μg/ml polyphyllin II according to group allocation. Images of the wounded area were captured at 0, 12 and 24 h using an inverted light microscope (DM2700M; Leica Microsystems GmbH). Cell migration was quantified by measuring the wound area at each time point using ImageJ software (version 1.53t, National Institutes of Health). The wound closure rate was calculated as follows: wound closure rate (%)=[(wound area at 0 h - wound area at indicated time point)/wound area at 0 h] x100. Each experiment was independently repeated at least three times.

Reverse transcription-quantitative (RT-q) PCR. TPC-1 and 8305C cells were seeded into six-well plates at a density of $2x10^5$ cells/well. After the indicated treatments, total RNA was extracted using RNAiso Plus reagent (Takara Bio, Inc.; cat. no. 9108) according to the manufacturer's protocol, and RNA concentration and purity were assessed via spectrophotometry. cDNA synthesis was performed using the designated reverse transcription kit (Takara Bio, Inc.; cat. no. RR047) according to the manufacturer's protocol. GAPDH was used as the internal control. The PCR cycling conditions were: Initial denaturation at 95˚C for 30 sec, followed by 40 cycles of denaturation at 95˚C for 5 sec and annealing/extension at 60˚C for 30 sec. qPCR was conducted using TB Green Premix Ex Taq II (Takara Bio, Inc.; cat. no. RR820A) on a real-time PCR detection system. The relative gene expression levels were calculated using the $2^{-\Delta\Delta Cq}$ method (13). Each experiment was independently repeated at least three times.

The primer sequences were: HRH1-F: GCAGGGACTATG TAGCCGTC; HRH1-R: GCCTGTGTTAGACCCACTCC; GAPDH-F: CAGGAGGCATTGCTGATGAT; GAPDH-R: GAAGGCTGGGGCTCATTT.

WB. Total cellular protein was extracted using RIPA lysis buffer (Beijing Solarbio Science & Technology Co., Ltd.; cat. no. R0010) containing protease and phosphatase inhibitors. Protein concentration was determined using a BCA protein assay kit (Beyotime Biotechnology; cat. no. P0010) according to the manufacture's protocol. The protein samples (30 μg/lane) were separated by 10% SDS-PAGE (Beijing Solarbio Science & Technology Co., Ltd.; cat. no. P1040), transferred to polyvinylidene difluoride membranes and blocked with 5% non-fat milk in Tris-buffered saline containing 0.1% Tween-20 (HuShi; cat. no. 30189328) for 1 h at room temperature. Subsequently, the membranes were incubated overnight at 4˚C with primary antibodies against HRH1 (Beyotime Biotechnology; cat. no. P70174),

Wnt7A (Beyotime Biotechnology; cat. no. AF8361), MMP7 (Beyotime Biotechnology; cat. no. AF7485), β-catenin (Beyotime Biotechnology; cat. no. AC106) and GAPDH (Beyotime Biotechnology; cat. no. AF0006). After washing with Tris-buffered saline containing 0.1% Tween-20, the membranes were incubated with HRP-conjugated goat anti-rabbit IgG secondary antibody (1:5,000; Beyotime Biotechnology; cat. no. A0208) or HRP-conjugated goat anti-mouse IgG secondary antibody (1:5,000; Beyotime Biotechnology; cat. no. A0216) for 1 h at room temperature. Protein bands were visualized using an enhanced chemiluminescence reagent (Beyotime Biotechnology) and quantified using ImageJ software (version 1.53t; National Institutes of Health). GAPDH was used as the loading control. Each experiment was independently repeated at least three times.

Molecular docking analysis. Molecular docking was performed to evaluate the potential interaction between polyphyllin II and HRH1. The chemical structure of polyphyllin II was obtained from the PubChem database, and the protein structure of HRH1 was obtained from the Protein Data Bank (https://www.rcsb.org/) or a predicted structural database. The ligand and receptor structures were prepared by removing water molecules, adding hydrogen atoms, and assigning charges. Docking analysis was then performed using AutoDock Vina (version 1.2.5, https://vina.scripps.edu/). The docking pose with the lowest binding energy was selected for further visualization, and the interaction between polyphyllin II and HRH1 was analyzed using PyMOL (version 2.5.4).

Drug Affinity Responsive Target Stability (DARTS) assay. To verify whether HRH1 is a potential target of the polyphyllin II, cell lysates were incubated with polyphyllin II or vehicle control, followed by pronase digestion. HRH1 protein levels were then detected by WB. Increased resistance of HRH1 to protease digestion indicated the interaction between polyphyllin II and HRH1.

Tumor xenograft model methodology. For the *in vivo* xenograft experiments, 8305C cells were selected as anaplastic thyroid carcinoma is more aggressive and clinically challenging and 8305C cells are suitable for evaluating tumor growth inhibition in a highly malignant thyroid cancer model. A total of 30 male BALB/c nude mice aged 4-6 weeks and weighing 18-22 g were purchased from Charles River Laboratories Co., Ltd. The mice were housed under specific pathogen-free conditions at 22±2˚C with 50-60% relative humidity and a 12-h light/dark cycle, with free access to food and water. Following 1 week of acclimatization, $1x10^6$ tumor cells were subcutaneous injected into the right dorsal flank of each mouse. Once tumor volumes approximately 100 mm^3, the mice were randomly assigned to five groups (n=6 per group), including TC, TC + polyphyllin II, NC, HRH1 knockdown (sh-HRH1) and HRH1 overexpression plus polyphyllin II treatment (OE HRH1 + polyphyllin II) groups. The control mice received intraperitoneal injections of vehicle solution (normal saline or DMSO diluent), while the treated mice were administered polyphyllin II (20 mg/kg/d) or subjected to lentiviral-mediated HRH1 modulation for 2-4 weeks. Tumor dimensions were measured every 2 days using vernier calipers and tumor volume was calculated as (length x $width^2$)/2 to generate growth curves.

Mice were monitored daily for general health status, behavior, food and water intake, body weight, tumor growth and tumor-related discomfort. Tumor dimensions were measured every 2 days using vernier calipers, and tumor volume was calculated as (length x $width^2$)/2. Humane endpoints were predefined as tumor volume >1,500 mm^3, tumor ulceration, necrosis or bleeding, impaired mobility, inability to access food or water, severe lethargy, persistent hunching, respiratory distress, or body weight loss >20% of baseline body weight. Mice that reached any humane endpoint were immediately sacrificed. At the end of the experiment, mice were deeply anesthetized with sodium pentobarbital at 50 mg/kg by intraperitoneal injection. Adequate depth of anesthesia was confirmed by the absence of pedal withdrawal and corneal reflexes. Cervical dislocation was then performed under deep anesthesia by trained personnel. Mortality was confirmed by the absence of respiration, heartbeat and reflex responses before tumor tissues were collected. All animal procedures were conducted in accordance with the ARRIVE guidelines and the AVMA Guidelines for the Euthanasia of Animals: 2020 Edition (https://www.avma.org/resources-tools/avma-policies/avma-guidelines-euthanasia-animals) and were approved by the Ethics Committee of The Fifth Affiliated Hospital of Kunming Medical University (approval no. kmmu20240805).

During the treatment period, mice were monitored daily for general health status, behavior, food and water intake, activity, body weight, tumor growth and tumor-related discomfort. No obvious treatment-related mortality or severe adverse effects were observed during the experimental period. Body weight was recorded regularly as a general indicator of systemic tolerability. The maximum tumor volume measured in this study was 880 mm^3, and the maximum tumor diameter did not exceed 12 mm.

Hematoxylin-eosin staining (H&E). Tumor tissues were fixed in 4% paraformaldehyde (Sinopharm Chemical Reagent Co., Ltd.; cat. no. 30525-89-4) for 24 h at room temperature. The tissues were dehydrated through a graded ethanol series (Sinoparm Chemical Reagent Co., Ltd.; cat. no. 100092683), including 70, 80, 90, 95 and 100% ethanol, cleared in xylene and embedded in paraffin (Sinoparm Chemical Reagent Co., Ltd.; cat. no. 1330-20-7). Paraffin-embedded tumor tissues were cut into 4-μm-thick sections. After deparaffinization and rehydration, the sections were stained with hematoxylin (Baso Diagnostics; cat. no. BA4097) for 5 min at room temperature and eosin (Baso Diagnostics; cat. no. BA4099) for 2 min at room temperature. The sections were then dehydrated, cleared, mounted with neutral resin and observed under a light microscope.

Immunohistochemical (IHC) evaluation of mouse tumor tissues. Immunohistochemical staining was performed on 4-μm-thick paraffin-embedded tumor tissue sections. After deparaffinization in xylene and rehydration through a graded ethanol series, antigen retrieval was performed by heating the sections in citrate antigen retrieval buffer at 95˚C for 15 min. Endogenous peroxidase activity was blocked with 3% hydrogen peroxide for 10 min at room temperature. The sections

were then blocked with 5% goat serum for 30 min at room temperature and incubated with anti-Ki67 antibody (Abcam; cat. no. ab16667; 1:300) overnight at 4˚C. After washing with phosphate-buffered saline, the sections were incubated with HRP-conjugated goat anti-rabbit IgG secondary antibody (Dako; Agilent Technologies, Inc.; cat. no. K4003, 1:500) for 30 min at room temperature. Immunoreactivity was visualized using a DAB chromogen detection kit, and the sections were counterstained with hematoxylin for 2 min at room temperature. Finally, the sections were dehydrated, cleared, mounted and observed under a light microscope. Images were acquired at x20 and x40 magnification.

Statistical analysis. All experiments were independently repeated at least three times. Data are presented as the mean ± standard deviation. Statistical analyses were performed using GraphPad Prism software version 9.0 (Dotmatics). The normality of data distribution was assessed using the Shapiro-Wilk test before applying parametric tests. For comparisons between two groups, Student's t-test was used for normally distributed data. For comparisons among multiple groups, one-way ANOVA followed by Tukey's post hoc test was performed. Spearman correlation analysis was used to evaluate the correlation between HRH1 expression and Wnt/β-catenin signaling pathway-related genes in The Cancer Genome Atlas-thyroid carcinoma dataset. Effect sizes were considered where appropriate to support the interpretation of biologically meaningful differences. $P<0.05$ was considered to indicate a statistically significant difference.

Results

Polyphyllin II suppresses thyroid cancer cell growth and motility. CCK-8 assays demonstrated that polyphyllin II markedly reduced the viability of thyroid cancer cells in a dose-dependent manner (Fig. 1A). Based on the IC_{50} value, it was ultimately determined that 5 μg/ml was the final experimental concentration. Flow cytometry analysis further revealed a significant increase in apoptotic cell populations following polyphyllin II treatment (Fig. 1B). Cell cycle analysis showed that polyphyllin II markedly increased the G_0/G_1-phase population in both 8305C and TPC-1 cells, while reducing the G_2/M-phase population. These results indicate that polyphyllin II induces G_0/G_1-phase cell cycle arrest, which may contribute to its anti-proliferative effect in thyroid cancer cells (Fig. 1C). Transwell invasion assays indicated that polyphyllin II attenuated the invasive capacity of 8305C and TPC-1 cells, whereas wound healing assays indicated impaired migratory ability following treatment (Fig. 1D and E). These findings indicate that polyphyllin II effectively restrains thyroid cancer progression by inhibiting proliferation and metastatic behavior.

Identification of HRH1 as a potential molecular target of polyphyllin II. Differential gene expression analysis revealed significant transcriptomic alterations in thyroid cancer, with 910 genes upregulated and 827 downregulated compared with non-tumor tissues (Fig. 2A). Target prediction using SwissTarget and intersection analysis identified 13 upregulated genes potentially associated with polyphyllin II (Fig. 2B and C). TCGA and GEO dataset validation confirmed that the expression levels of HRH1, LGALS1, ADORA1 and ECE1 were significantly elevated in thyroid cancer (Fig. 2D and E). Among these genes, HRH1 has been reported as an oncogenic mediator in multiple cancer types through regulation of cell survival, angiogenesis, immune modulation and invasion (14,15), suggesting its potential role in thyroid cancer progression.

HRH1 is overexpressed in thyroid cancer cells. RT-qPCR analysis confirmed that the expression levels of HRH1, LGALS1, ADORA1 and ECE1 were markedly upregulated in thyroid cancer cells (Fig. 3A). Western blotting further validated elevated protein levels of these targets, with HRH1 indicating notably high expression in TPC-1 and 8305C cells (Fig. 3B). Given that HRH1 signaling mediates histamine-induced tumor proliferation and immune escape across multiple malignancies, HRH1 was selected as the primary candidate for further investigation.

Polyphyllin II directly interacts with HRH1 and regulates HRH1 expression. To determine whether HRH1 is a direct target of polyphyllin II, molecular docking and DARTS assays were performed. Molecular docking showed that polyphyllin II could fit into the predicted binding pocket of HRH1, suggesting a potential interaction between polyphyllin II and HRH1 (Fig. 4A). Consistently, DARTS assay showed that polyphyllin II increased the resistance of HRH1 protein to pronase digestion, further supporting the direct interaction between polyphyllin II and HRH1 (Fig. 4B).

The present study next modulated HRH1 expression in thyroid cancer cells. RT-qPCR and western blot results confirmed that sh-HRH1 significantly reduced HRH1 expression, whereas OE-HRH1 markedly increased HRH1 expression (Fig. 4C-F). These results indicated that HRH1 can be directly targeted by polyphyllin II and that the HRH1 knockdown and overexpression models were successfully established for subsequent functional experiments.

HRH1 silencing attenuates the malignant phenotype of thyroid cancer cells. To determine the functional role of HRH1 in thyroid cancer cells, HRH1 was silenced using sh-HRH1. CCK-8 assays showed that HRH1 knockdown significantly reduced the proliferation of both 8305C and TPC-1 cells compared with the control and sh-NC groups (Fig. 5A and B). Flow cytometry further showed that sh-HRH1 increased the apoptosis rate in both cell lines (Fig. 5C). In addition, Transwell assays demonstrated that HRH1 knockdown markedly decreased the invasive ability of 8305C and TPC-1 cells (Fig. 5D). Wound-healing assays also showed that sh-HRH1 delayed wound closure, indicating impaired migratory capacity after HRH1 silencing (Fig. 5E). These results suggest that HRH1 promotes malignant phenotypes in thyroid cancer cells.

Polyphyllin II exerts its antitumor effects via HRH1 suppression. Overexpression of HRH1 counteracted apoptosis and enhanced invasive and migratory abilities in TPC-1 and 8305C cells, whereas polyphyllin II administration reversed these effects (Fig. 6A-E). These results suggest that polyphyllin II inhibits

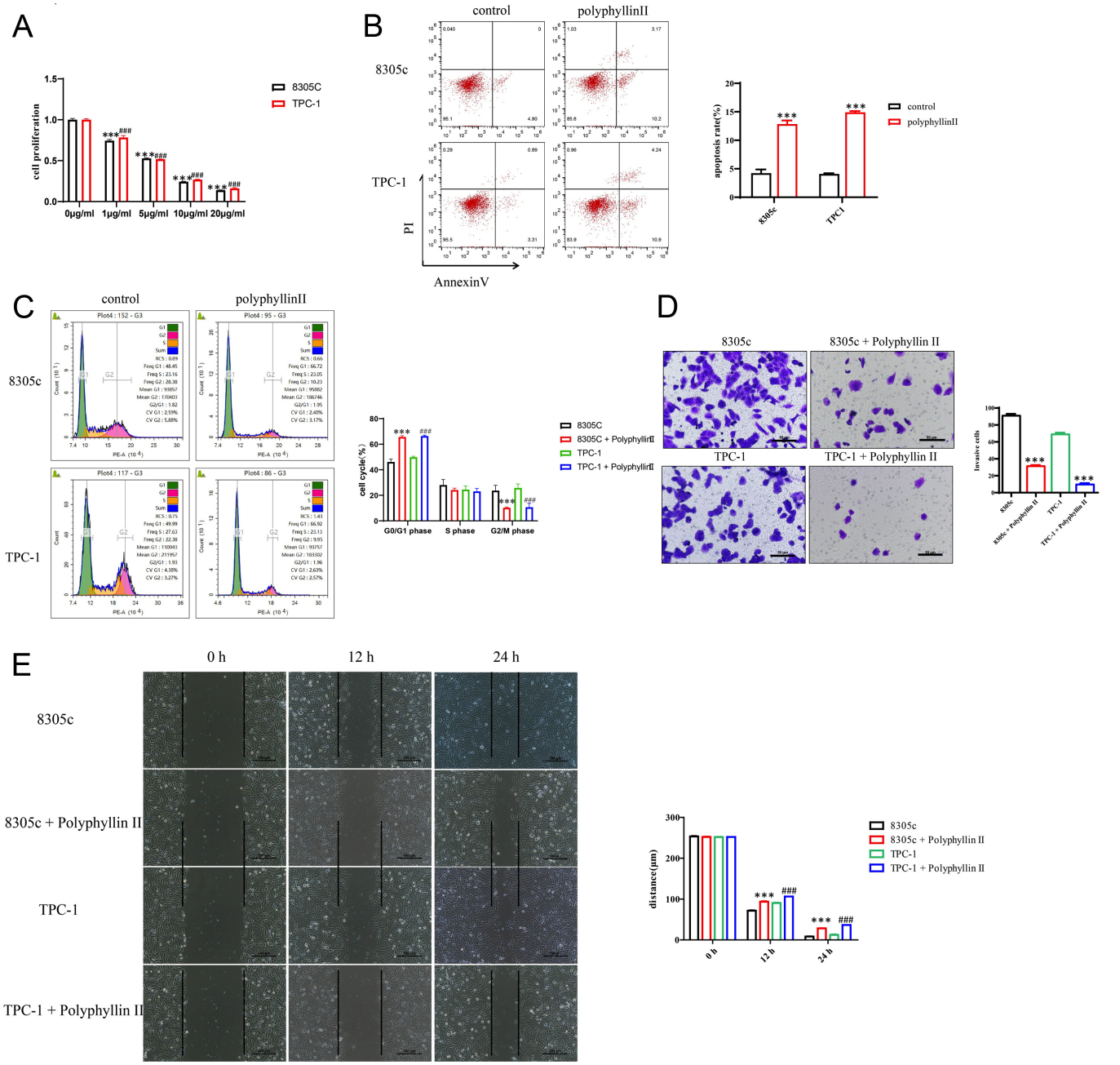

Figure 1. Polyphyllin II inhibits proliferation, invasion, and migration and induces apoptosis in thyroid cancer cells. (A) CCK-8 assay showing reduced viability of 8305C and TPC-1 cells after treatment with increasing concentrations of polyphyllin II for 24 h. (B) Flow cytometry analysis of Annexin V-FITC/PI-stained cells indicating enhanced apoptosis following polyphyllin II exposure. (C) Flow cytometry-based cell cycle experiment. (D) Transwell invasion assay showing decreased number of invaded cells after treatment. Scale bar, 50 μm. (E) Wound-healing assay showing impaired migratory ability in polyphyllin II-treated cells at 0, 12 and 24 h. Data are presented as mean ± SD (n=3). ***P<0.01 vs. 8305C control. $^{###}$P<0.001 vs. TPC-1 control.FITC, fluorescein isothiocyanate.

thyroid cancer malignancy in part by attenuating HRH1 signaling. Given that HRH1 acts as a downstream regulator of histamine signaling and oncogenic activity, these findings provide a mechanistic basis for using polyphyllin II as a potential HRH1-targeted therapeutic strategy.

HRH1 regulates Wnt/β-catenin signaling and polyphyllin II reverses its activation. Previous evidence suggests that histamine receptor H1-related signaling may activate canonical β-catenin signaling, while Wnt/β-catenin activation is closely associated with thyroid cancer progression (16-18). Consistently, TCGA-THCA single-gene correlation analysis showed that HRH1 was positively correlated with several Wnt/β-catenin-related genes, including MMP7, WNT7A, CCND1, TCF7, CTNNB1 and MYC (Fig. S1). These findings provided a rationale for subsequent experimental validation. Knockdown of HRH1 expression significantly reduced the expression levels of the β-catenin pathway-related genes (MMP7, Wnt7A and β-catenin) and decreased β-catenin nuclear translocation, whereas polyphyllin II treatment further suppressed pathway activation (Fig. 7A and B). Conversely, HRH1 overexpression enhanced β-catenin signaling, while polyphyllin II blocked this activation, indicating an HRH1-dependent regulatory mechanism. Therefore,

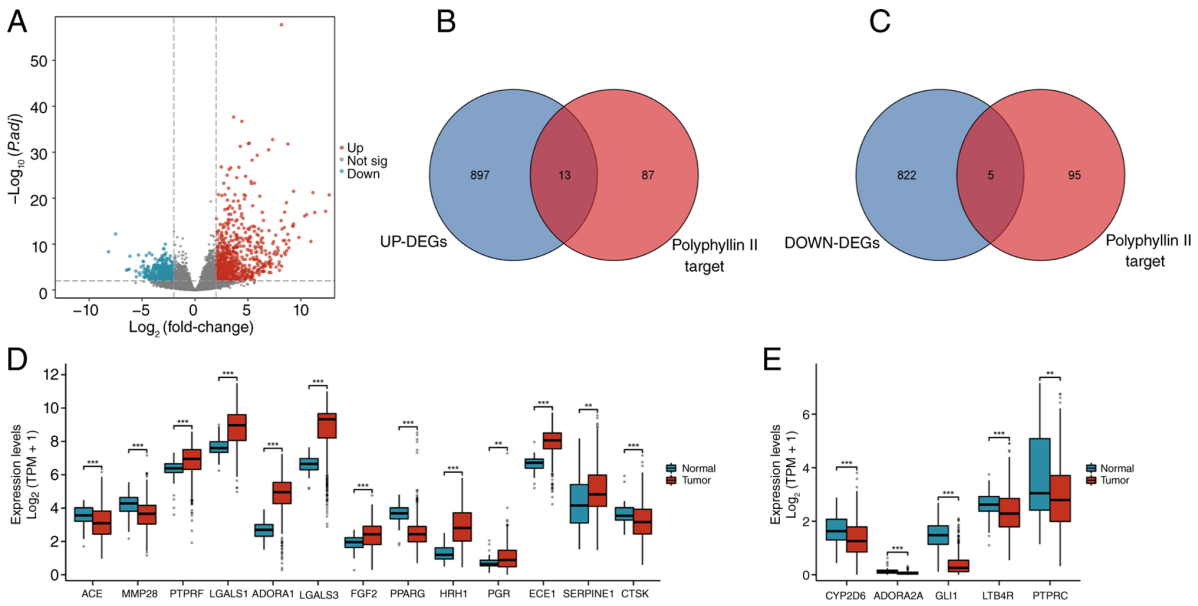

Figure 2. Identification of HRH1 as a potential target of polyphyllin II based on differential expression and target prediction analyses. (A) Volcano plot of differentially expressed genes (GSE197443) between thyroid cancer and normal tissues. (B and C) Venn diagrams showing overlap between predicted polyphyllin II-associated genes and differentially upregulated/downregulated genes in thyroid cancer. (D and E) TCGA analysis validating upregulated HRH1, LGALS1, ADORA1 and ECE1 expression in thyroid carcinoma. Red indicates upregulation; blue indicates downregulation. HRH1, histamine receptor H1; TCGA, The Cancer Genome Atlas. **P<0.01 and ***P<0.001 vs. normal tissues.

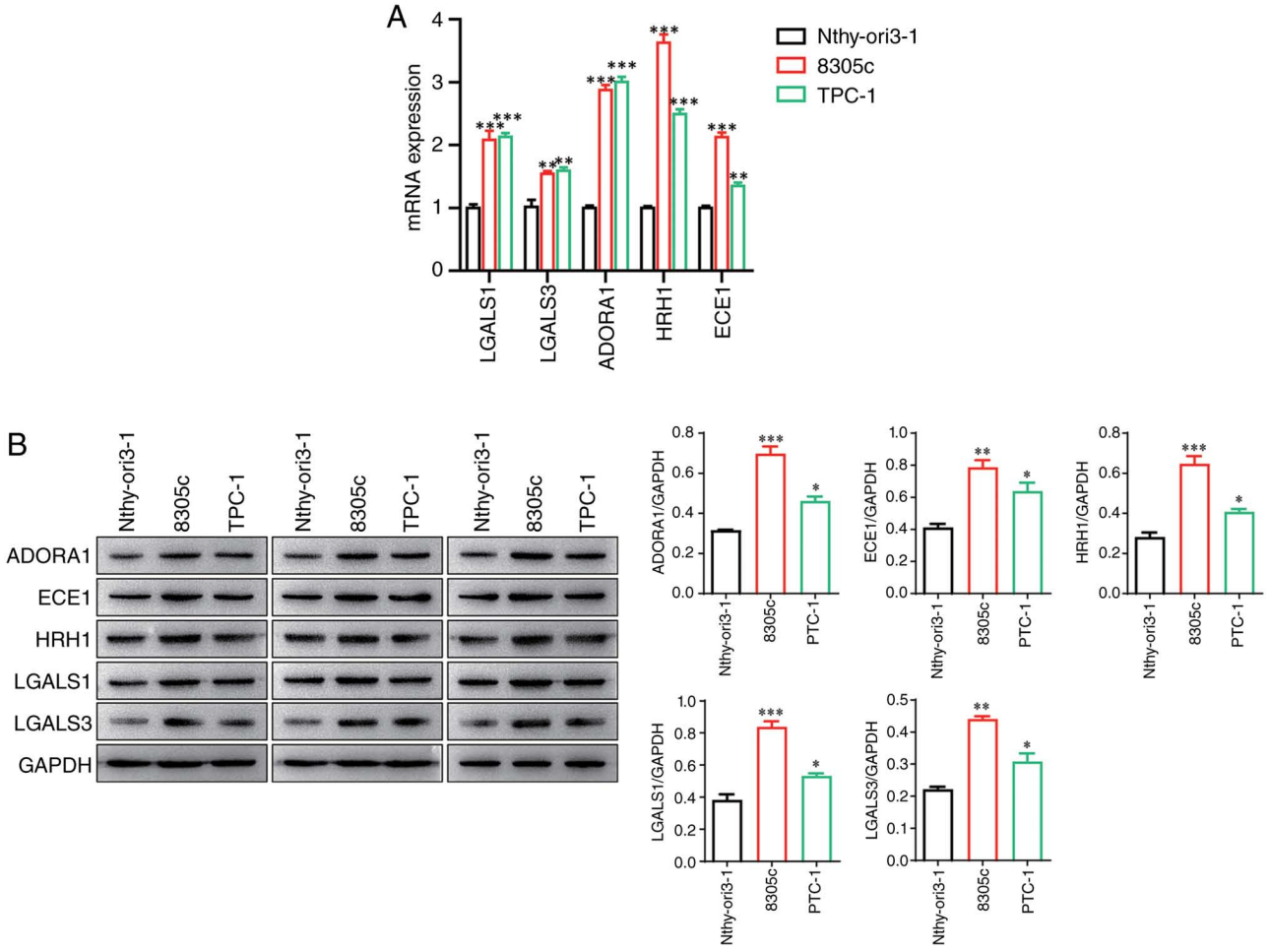

Figure 3. HRH1 is highly expressed in thyroid cancer cells. (A) RT-qPCR validation of HRH1, LGALS1, ADORA1 and ECE1 gene expression in TPC-1, 8305C, and Nthy-ori 3-1 cells. (B) Western blotting detection of corresponding protein expression levels. GAPDH served as internal control. Quantification is shown as mean ± SD (n=3). *P<0.05, **P<0.01, ***P<0.001 vs. Nthy-ori-3-1 group. HRH1, histamine receptor H1; RT-qPCR, reverse transcription quantitative PCR.

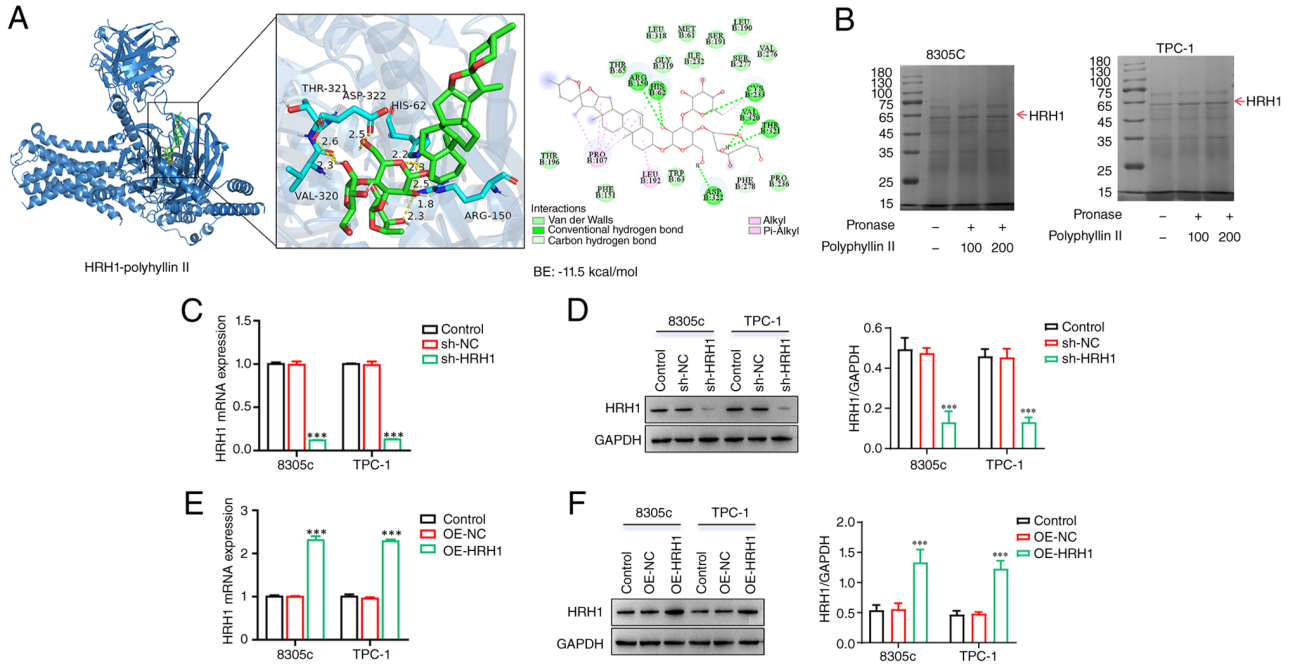

Figure 4. Polyphyllin II directly interacts with HRH1 and successful modulation of HRH1 expression in thyroid cancer cells. (A) Molecular docking analysis showing the predicted binding mode of polyphyllin II with HRH1. The binding pocket, interacting residues and 2D interaction diagram are shown, with a predicted binding energy of -11.5 kcal/mol. (B) DARTS assay showing that polyphyllin II increased the resistance of HRH1 protein to pronase digestion in 8305C and TPC-1 cells, supporting a potential interaction between polyphyllin II and HRH1. (C) RT-qPCR confirming the knockdown efficiency of sh-HRH1 in 8305C and TPC-1 cells. (D) Western blotting and quantification showing reduced HRH1 protein expression after sh-HRH1 transduction. (E) RT-qPCR confirming the overexpression efficiency of OE-HRH1 in 8305C and TPC-1 cells. (F) Western blot analysis and quantification showing increased HRH1 protein expression after OE-HRH1 transduction. GAPDH was used as the loading control. Data are presented as the mean ± SD (n=3). ***P<0.001 vs. sh-NC or OE-NC group. HRH1, histamine receptor H1; DARTS, Drug Affinity Responsive Target Stability; RT-qPCR, reverse transcription quantitative PCR; sh, short hairpin; OE, overexpression; NC, negative control.

polyphyllin II may exert antitumor effects in thyroid cancer by suppressing HRH1-mediated β-catenin activation.

Treatment of thyroid cancer cells with polyphyllin II in vivo. To validate the *in vivo* findings, xenograft models were established using 8305C cells in nude mice. The growth transplanted 8305C xenograft tumors in mice was accelerated significantly. During the *in vivo* treatment period, no obvious treatment-related toxicity was observed. Mice in the polyphyllin II-treated group showed no marked abnormalities in general behavior, activity, food intake or water intake. Body weight remained relatively stable throughout the experiment, suggesting that polyphyllin II was generally tolerated under the present treatment conditions. The mice that were treated with polyphyllin II demonstrated a significant reduction in tumor size, indicating that polyphyllin II exhibited an inhibitory effect on tumors (Fig. 8A-D). The tumor tissues were stained using IHC analysis for H&E and Ki67. The results indicated that polyphyllin II could alleviate the deterioration of the tumor tissues and reduce cancer cell proliferation (Fig. 8E and F). WB results indicated that the expression levels of the proteins of the HRH1 signaling pathway were reduced following the use of polyphyllin II (Fig. 8G).

To further confirm the effect of polyphyllin II on the HRH1 signaling pathway, 8305C cells were divided into three groups; NC, lentiviral sh-HRH1 and lentiviral OE-HRH1 combined with polyphyllin II treatment. Compared with NC, following knockdown of HRH1 expression, the tumor size decreased. Following IHC staining with H&E and Ki67, the severity of tumor tissue deterioration decreased and the proliferation of the cells was reduced (Fig. 9A-D). Following treatment of the tumor-bearing mice expressing HRH1 with polyphyllin II, the volumes of the tumors were reduced. The tissue staining results indicated that the severity of tumor tissue deterioration and cellular proliferation were reduced (Fig. 9E and F). WB results also demonstrated that polyphyllin II inhibited tumor growth by suppressing the HRH1 signaling pathway (Fig. 9G).

Discussion

Thyroid cancer remains a heterogeneous endocrine malignancy and aggressive or treatment-resistant subtypes still require more effective molecular therapeutic strategies. In the present study, polyphyllin II inhibited proliferation, invasion and migration, while promoting apoptosis in thyroid cancer cells. Mechanistically, HRH1 was identified as a potential target of polyphyllin II, and HRH1 suppression was associated with reduced activation of the Wnt/β-catenin pathway. These findings suggested that the HRH1/Wnt/β-catenin axis may contribute to thyroid cancer progression and may serve as a potential therapeutic target.

HRH1 is a histamine receptor involved in inflammatory signaling, cell proliferation and tumor progression. Previous evidence has shown that histamine can activate the canonical β-catenin pathway through H1 receptor-dependent regulation of glycogen synthase kinase-3β activity and β-catenin stabilization (19). To further support this potential link in thyroid

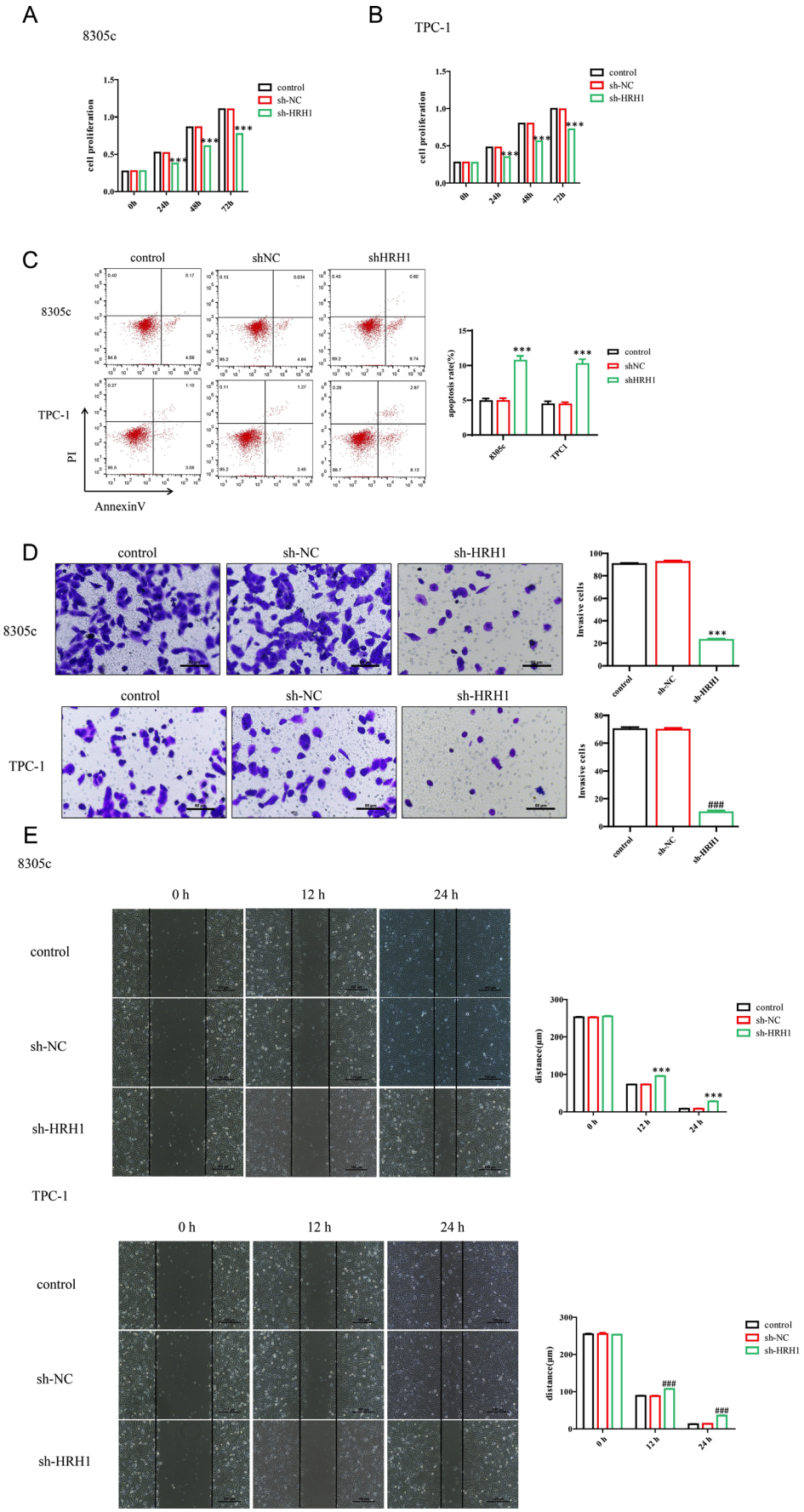

Figure 5. HRH1 knockdown suppresses proliferation, invasion, and migration, and induces apoptosis in thyroid cancer cells. (A and B) Reduced proliferation capacity following HRH1 knockdown measured by CCK-8. (C) Flow cytometry showing increased apoptosis in sh-HRH1-transduced cells. (D) Transwell invasion analysis showing reduced invasive ability after HRH1 silencing. Scale bar, 50 μm. (E) Wound-healing assay indicating reduced migration following HRH1 knockdown. Data are shown as mean ± SD (n=3). ***P<0.001 vs. control. $^{###}$P<0.001 vs. sh-NC. HRH1, histamine receptor H1; CCK-8, Cell Counting Kit-8; sh, short hairpin; NC, negative control.

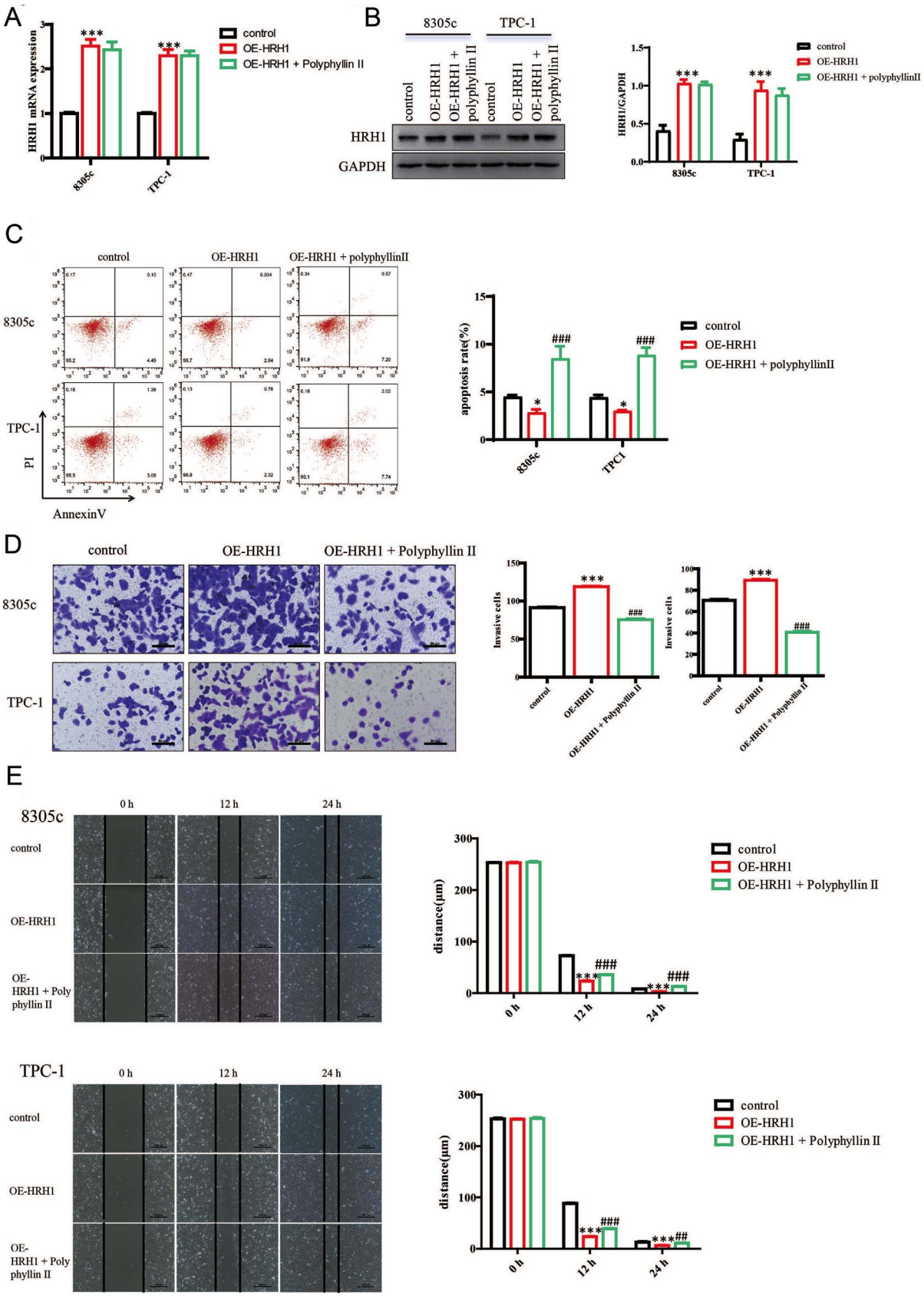

Figure 6. Polyphyllin II inhibits HRH1-mediated malignant phenotypes in thyroid cancer cells. (A) RT-qPCR showing HRH1 mRNA expression in control, OE-HRH1 and OE-HRH1 + polyphyllin II groups in 8305C and TPC-1 cells. (B) Western blotting and quantification of HRH1 protein expression in 8305C and TPC-1 cells. GAPDH was used as the loading control. (C) Flow cytometry analysis of Annexin V/PI staining showing that HRH1 overexpression reduced apoptosis, whereas polyphyllin II treatment increased apoptosis in HRH1-overexpressing cells. (D) Transwell invasion assay showing that HRH1 overexpression enhanced the invasive ability of 8305C and TPC-1 cells, while polyphyllin II treatment suppressed HRH1-induced invasion. Scale bar, 50 μm. (E) Wound-healing assay showing that HRH1 overexpression promoted cell migration at 12 and 24 h, whereas polyphyllin II treatment attenuated HRH1-induced migratory capacity. Data are presented as the mean ± SD (n=3). *P<0.05 and ***P<0.001 vs. control group. $^{###}$P<0.001 vs. OE-HRH1 group. HRH1, histamine receptor H1; RT-qPCR, reverse transcription quantitative PCR; OE, overexpression; PI, propidium iodide.

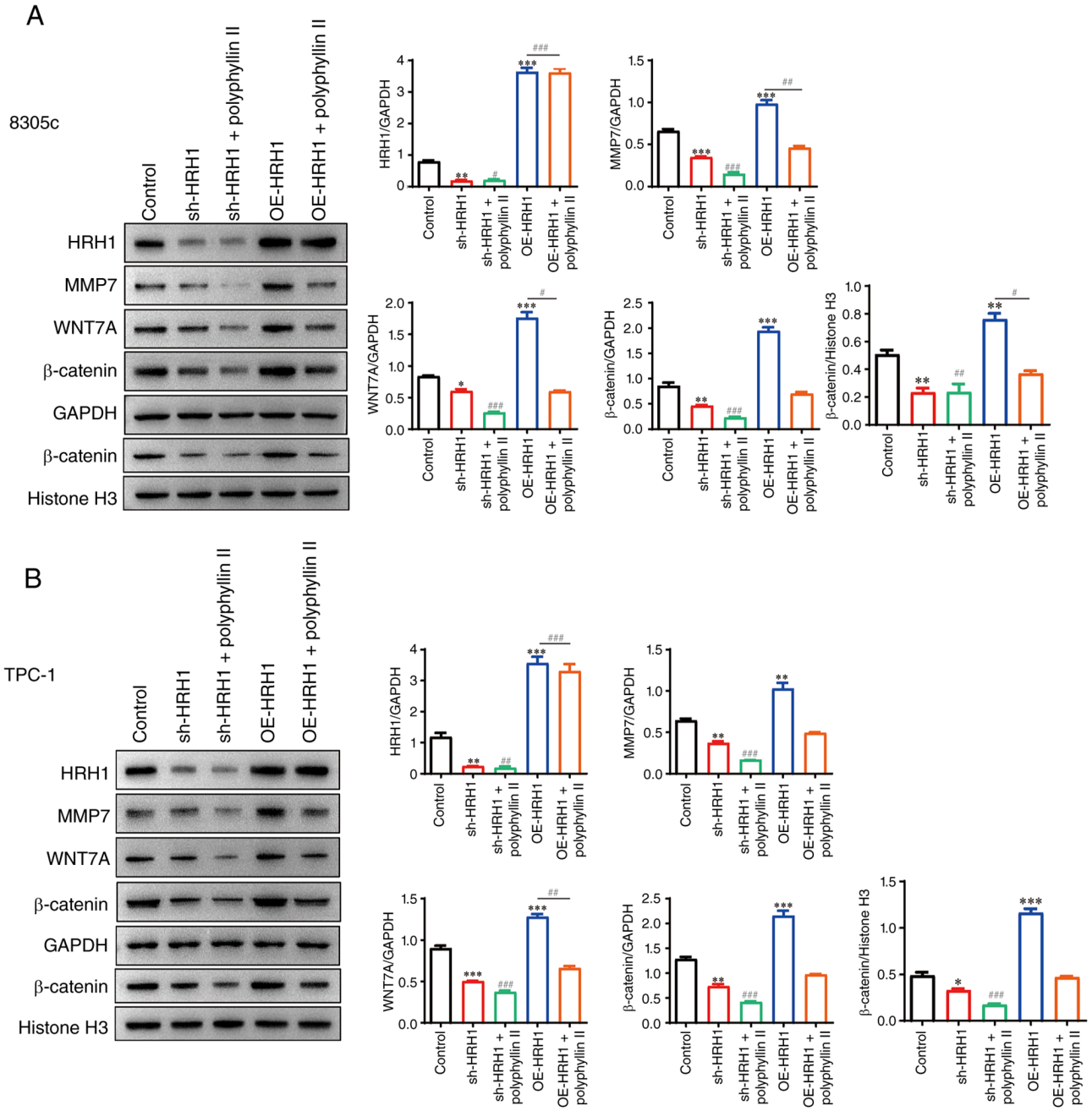

Figure 7. Polyphyllin II suppresses HRH1-induced activation of the Wnt/β-catenin signaling pathway. (A) Western blotting showing reduced expression of β-catenin, MMP7 and WNT7A after HRH1 knockdown and further suppression following polyphyllin II treatment. (B) Nuclear and cytoplasmic fractionation western blotting demonstrating decreased β-catenin nuclear localization after polyphyllin II treatment in HRH1-overexpressing cells. Lamin B and GAPDH served as nuclear and cytoplasmic markers, respectively. Quantification is shown as mean ± SD (n=3). *P<0.05 and **P<0.01, ***P<0.001 vs. control group; $^{\#}$P<0.05 and $^{\#\#}$P<0.01, $^{\#\#\#}$P<0.001 vs. the corresponding control group, including sh-NC for sh-HRH1 comparisons and OE-HRH1 for OE-HRH1 + polyphyllin II comparisons. HRH1, histamine receptor H1; OE, overexpression; sh, short hairpin; NC, negative control.

cancer, the present study performed single-gene correlation analysis using the TCGA-THCA dataset. The results showed that HRH1 expression was positively correlated with several Wnt/β-catenin-related genes, including MMP7, WNT7A, CCND1, TCF7, CTNNB1 and MYC. These literature and bioinformatics findings provided a rationale for further investigating whether HRH1 regulates Wnt/β-catenin signaling in thyroid cancer cells.

Wnt/β-catenin signaling is an important oncogenic pathway involved in thyroid cancer proliferation, invasion, dedifferentiation and treatment resistance (20-22). In the present study, HRH1 knockdown reduced the expression of β-catenin pathway-related molecules, whereas HRH1 overexpression enhanced pathway activation. Notably, polyphyllin II attenuated HRH1-mediated activation of Wnt/β-catenin signaling, suggesting that its antitumor effect may be partly dependent on inhibition of the HRH1/Wnt/β-catenin axis. These findings indicated that polyphyllin II may not act merely as a cytotoxic compound, but may suppress thyroid cancer progression through a defined HRH1/Wnt/β-catenin signaling axis. This also raises the possibility that polyphyllin II could be further explored in combination with agents targeting

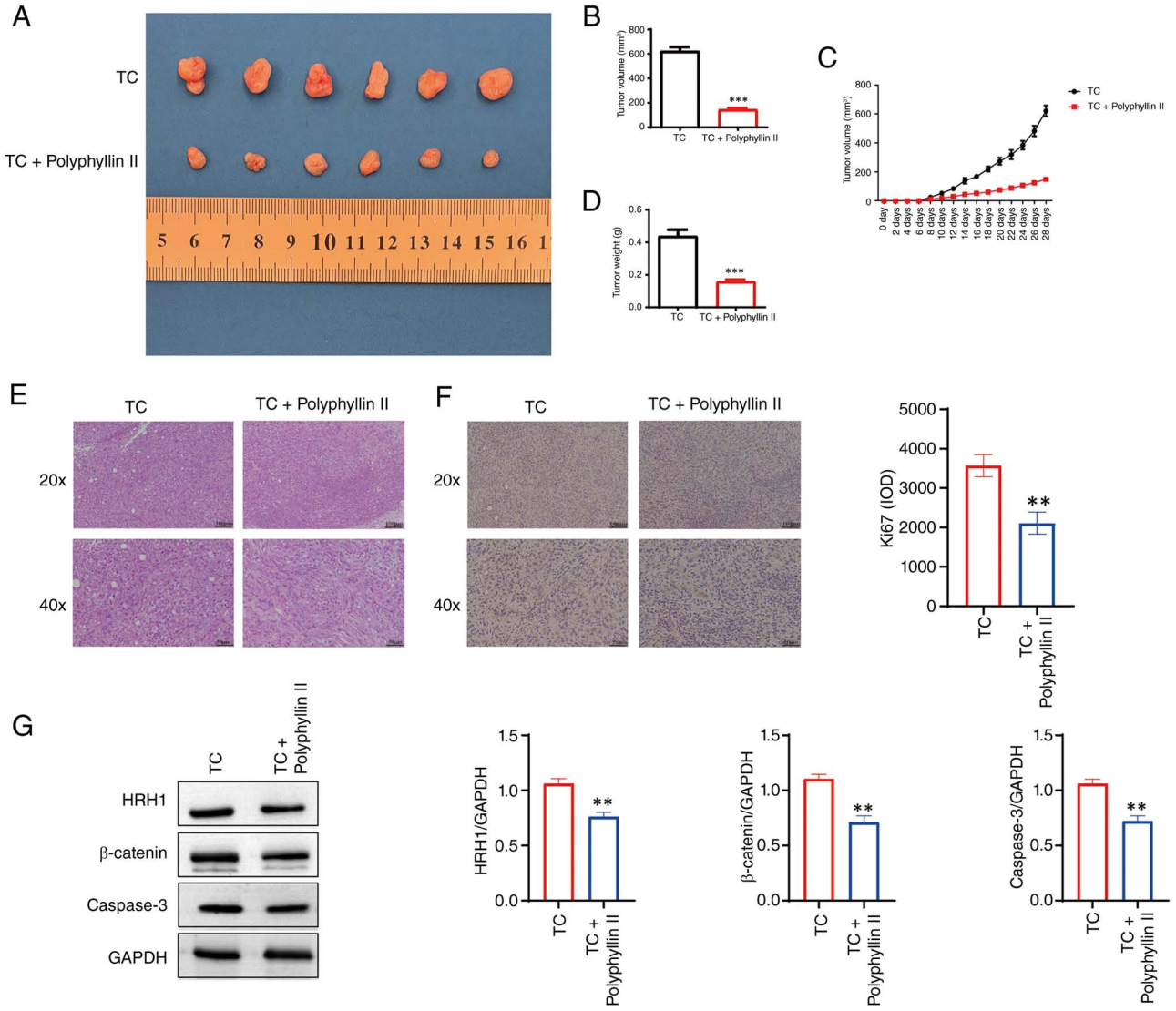

Figure 8. Polyphyllin II inhibits tumor growth *in vivo*. (A) Representative images of xenograft tumors from the TC and TC + polyphyllin II groups. (B and C) Quantitative analysis of tumor volume and tumor weight showing that polyphyllin II significantly reduced xenograft tumor burden. (D) Tumor growth curves showing that polyphyllin II treatment markedly suppressed tumor growth over time. (E) H&E staining of tumor tissues showing reduced tumor cell density and improved histological morphology after polyphyllin II treatment. (F) Immunohistochemical staining and quantitative analysis of Ki67 showing decreased tumor cell proliferation in the polyphyllin II-treated group. Scale bar, 100 μm for images acquired at x20 magnification and 50 μm for images acquired at x40 magnification. (G) Western blot analysis and quantification of HRH1, β-catenin and caspase-3 protein expression in xenograft tumor tissues. GAPDH was used as the loading control. Data are presented as the mean ± SD (n=6). **P<0.01 and ***P<0.001 vs. TC group. TC, thyroid cancer; H&E, hematoxylin-eosin; HRH1, histamine receptor H1.

the Wnt/β-catenin pathway, particularly in aggressive or treatment-resistant thyroid cancer.

From a clinical perspective, these findings may have potential relevance for biomarker-based risk stratification in thyroid cancer. Current endocrine surgical practice increasingly emphasizes the integration of imaging, cytology, molecular markers and systemic inflammatory indicators to improve the evaluation of thyroid nodules and tumor aggressiveness (23,24). Gambardella *et al* (7) reported that inflammatory biomarkers, including neutrophil-to-lymphocyte ratio, lymphocyte-to-monocyte ratio and platelet-to-lymphocyte ratio, may help predict malignancy in indeterminate thyroid nodules. As an inflammation-related receptor, HRH1 may provide a molecular link between inflammatory regulation and oncogenic signaling in thyroid cancer. Therefore, HRH1-related signaling may have potential value for further evaluating tumor behavior and identifying patients who may benefit from pathway-oriented therapeutic strategies.

The translational relevance of the present study should also be considered in the context of multimodal management for aggressive thyroid cancer. For highly aggressive subtypes, particularly anaplastic thyroid carcinoma, surgery alone is often insufficient, and combined strategies involving surgery, radiotherapy, chemotherapy and systemic treatment are frequently required. Conzo *et al* (25) emphasized the importance of multimodal treatment in improving local control and clinical outcomes in selected patients with aggressive thyroid cancer. In this context, the HRH1/Wnt/β-catenin axis identified in the present study may provide a molecular basis for future combination strategies. Although polyphyllin II remains a preclinical candidate, its inhibitory effect on HRH1-mediated Wnt/β-catenin

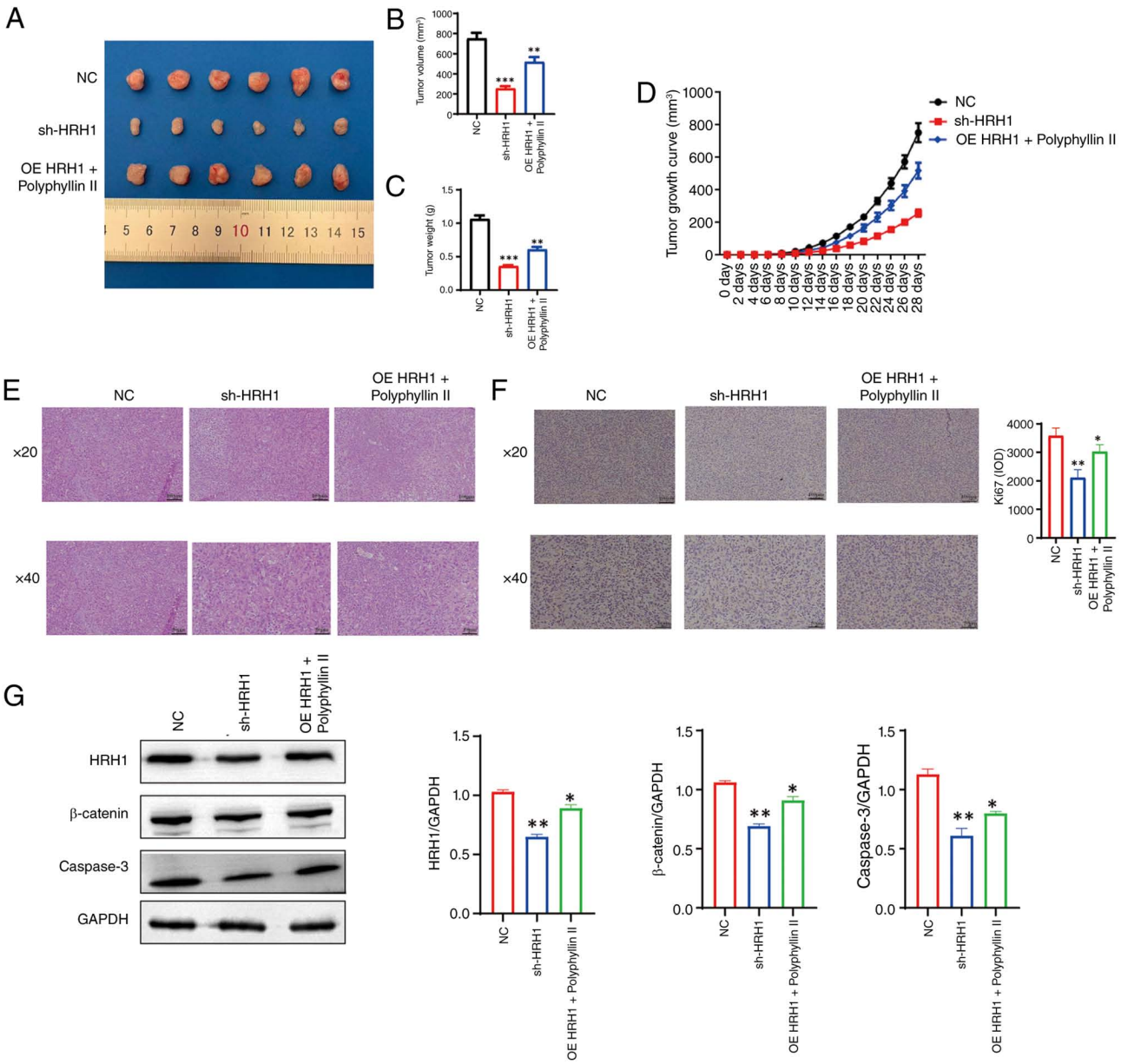

Figure 9. HRH1 modulation affects xenograft tumor growth and polyphyllin II suppresses HRH1-mediated tumor progression *in vivo*. (A) Representative images of xenograft tumors from the NC, sh-HRH1, and OE-HRH1 + polyphyllin II groups. (B and C) Quantitative analysis of tumor volume and tumor weight showing that HRH1 knockdown significantly reduced tumor burden, while polyphyllin II treatment also suppressed tumor growth in HRH1-overexpressing xenografts. (D) Tumor growth curves showing reduced tumor progression in the sh-HRH1 group and the OE-HRH1 + polyphyllin II group compared with the NC group. (E) H&E staining of xenograft tumor tissues showing decreased tumor cell density and improved histological morphology after HRH1 knockdown or polyphyllin II treatment. (F) Immunohistochemical staining and quantitative analysis of Ki67 showing reduced tumor cell proliferation in the sh-HRH1 and OE-HRH1 + polyphyllin II groups. Scale bar=100 μm for images acquired at x20 magnification and 50 μm for images acquired at x40 magnification. (G) Western blotting and quantification of HRH1, β-catenin and caspase-3 expression in xenograft tumor tissues. GAPDH was used as the loading control. Data are presented as the mean ± SD (n=6). *P<0.05, **P<0.01 and ***P<0.001 vs. NC group. HRH1, histamine receptor H1; sh, short hairpin; OE, overexpression; NC, negative control; H&E, hematoxylin-eosin.

activation suggests that it may have potential value as part of pathway-oriented therapeutic exploration.

The broader surgical literature also indicates that clinical outcomes are influenced not only by local disease control, but also by systemic metabolic status and perioperative management. Studies by Pizza *et al* (26-28) in metabolic surgery showed that postoperative metabolic modulation, antral size and biliopancreatic limb length may affect postoperative complications, nutritional status and long-term outcomes. Therefore, future translational studies of thyroid cancer should not only focus on tumor-intrinsic molecular pathways, but also consider inflammatory status, metabolic background, surgical risk and postoperative recovery.

Several limitations should be acknowledged. First, although xenograft experiments were performed in the present study, the *in vivo* regulatory relationship among polyphyllin II, HRH1 and Wnt/β-catenin signaling requires further validation using more clinically relevant models, such as orthotopic thyroid cancer models or patient-derived xenografts. Second, the upstream mechanisms responsible for HRH1 overexpression in thyroid

cancer were not fully explored. Future studies should examine whether inflammatory mediators, epigenetic regulation, histamine-related metabolic changes or tumor microenvironmental signals contribute to HRH1 activation. Moreover, it remains possible that polyphyllin II may also affect other components of the Wnt/β-catenin pathway, including Frizzled receptors, low-density lipoprotein receptor-related protein 5/6 (LRP5/6), GSK3β, β-catenin and TCF/LEF transcriptional complexes. Future studies should evaluate whether polyphyllin II directly interacts with these Wnt/β-catenin-related targets or indirectly suppresses the pathway through HRH1-dependent regulation. Third, although molecular docking and DARTS assays supported a potential interaction between polyphyllin II and HRH1, additional target-engagement assays, such as surface plasmon resonance or cellular thermal shift assays, would further strengthen the evidence for direct binding. Finally, given the important role of Wnt/β-catenin signaling in thyroid cancer progression and treatment resistance, future studies should investigate whether polyphyllin II can be combined with Wnt/β-catenin pathway inhibitors, targeted therapies or conventional treatments to enhance antitumor efficacy.

In conclusion, the present study demonstrated that polyphyllin II suppresses thyroid cancer progression by targeting HRH1 and inhibiting Wnt/β-catenin signaling. These findings provided new insight into the role of HRH1-related signaling in thyroid cancer and suggested that HRH1 may serve as a potential therapeutic target. Further studies are needed to validate the clinical relevance of HRH1 and to explore polyphyllin II-based combination strategies for aggressive or treatment-resistant thyroid cancer.

Acknowledgements

Not applicable.

Funding

The present study was supported by funds from Yunnan Provincial Department of Science and Technology, Key Project for Applied Basic Research (Yunnan Fundamental Research Kunming Medical University Projects; grant no. 202301AY070001-037), Yunnan Province 'Xingdian Talents' Support Program for Healthcare Professionals (grant no. XDYC-MY-2022-070) and China Health Promotion Foundation, Key Project of the Research Fund for High-Quality Development of Public Hospitals (grant no. GL-A013).

Availability of data and materials

The data generated in the present study may be requested from the corresponding author.

Authors' contributions

JS was responsible for manuscript writing and revision, cellular experiments and molecular mechanistic studies. HL and YZ were responsible for cellular experiments. DD and QX were responsible for manuscript revision. MZ was responsible for clinical research. PZ was responsible for overall design and direction of the dissertation. JS and PZ confirm the authenticity of all the raw data. All authors read and approved the final manuscript.

Ethics approval and consent to participate

All animal procedures were conducted in accordance with the ARRIVE guidelines and the AVMA Guidelines for the Euthanasia of Animals: 2020 Edition and were approved by the Ethics Committee of The Fifth Affiliated Hospital of Kunming Medical University (approval no. kmmu20240805).

Patient consent for publication

Not applicable.

Competing interests

The authors declare that they have no competing interests.

References

1. Megwalu UC and Moon PK: Thyroid cancer incidence and mortality trends in the United States: 2000-2018. Thyroid 32: 560-570, 2022.
2. Cabanillas ME, McFadden DG and Durante C: Thyroid cancer. Lancet 388: 2783-2795, 2016.
3. Haugen BR, Alexander EK, Bible KC, Doherty GM, Mandel SJ, Nikiforov YE, Pacini F, Randolph GW, Sawka AM, Schlumberger M, *et al*: 2015 American thyroid association management guidelines for adult patients with thyroid nodules and differentiated thyroid cancer: The American thyroid association guidelines task force on thyroid nodules and differentiated thyroid cancer. Thyroid 26: 1-133, 2016.
4. Parker WA, Edafe O and Balasubramanian SP: Long-term treatment-related morbidity in differentiated thyroid cancer: A systematic review of the literature. Pragmat Obs Res 8: 57-67, 2017.
5. Rao SN and Smallridge RC: Anaplastic thyroid cancer: An update. Best Pract Res Clin Endocrinol Metab 37: 101678, 2023.
6. Spitzweg C, Bible KC, Hofbauer LC and Morris JC: Advanced radioiodine-refractory differentiated thyroid cancer: The sodium iodide symporter and other emerging therapeutic targets. Lancet Diabetes Endocrinol 2: 830-842, 2014.
7. Gambardella C, Mongardini FM, Paolicelli M, Bentivoglio D, Cozzolino G, Ruggiero R, Pizza A, Tolone S, Del Genio G, Parisi S, *et al*: Role of inflammatory biomarkers (NLR, LMR, PLR) in the prognostication of malignancy in indeterminate thyroid nodules. Int J Mol Sci 24: 6466, 2023.
8. Cheong TY, Hong SD, Jung KW and So YK: The diagnostic predictive value of neutrophil-to-lymphocyte ratio in thyroid cancer adjusted for tumor size. PLoS One 16: e0251446, 2021.
9. Ding YG, Zhao YL, Zhang J, Zuo ZT, Zhang QZ and Wang YZ: The traditional uses, phytochemistry, and pharmacological properties of Paris L. (Liliaceae): A review. J Ethnopharmacol 278: 114293, 2021.
10. Carnazza M, Yang N, Tiwari RK, Geliebter J and Li XM: Natural compounds targeting MAPK, PI3K/Akt, and JAK/STAT signaling in papillary thyroid cancer. Int J Mol Sci 26: 10498, 2025.
11. Li JK, Sun HT, Jiang XL, Chen YF, Zhang Z, Wang Y, Chen WQ, Zhang Z, Sze SCW, Zhu PL and Yung KKL: Polyphyllin II induces protective autophagy and apoptosis via inhibiting PI3K/AKT/mTOR and STAT3 signaling in colorectal cancer cells. Int J Mol Sci 23: 11890, 2022.
12. Miao W, Wang Z, Gao J and Ohno Y: Polyphyllin II inhibits breast cancer cell proliferation via the PI3K/Akt signaling pathway. Mol Med Rep 30: 224, 2024.
13. Livak KJ and Schmittgen TD: Analysis of relative gene expression data using real-time quantitative PCR and the 2(-Delta Delta C(T)) method. Methods 25: 402-408, 2001.
14. Zhao J, Hou Y, Yin C, Hu J, Gao T, Huang X, Zhang X, Xing J, An J, Wan S and Li J: Upregulation of histamine receptor H1 promotes tumor progression and contributes to poor prognosis in hepatocellular carcinoma. Oncogene 39: 1724-1738, 2020.

15. Ding YF, Ho KH, Lee WJ, Chen LH, Hsieh FK, Tung MC, Lin SH, Hsiao M, Yang SF, Yang YC and Chien MH: Cyclic increase in the histamine receptor H1-ADAM9-Snail/Slug axis as a potential therapeutic target for EMT-mediated progression of oral squamous cell carcinoma. Cell Death Dis 16: 191, 2025.
16. Diks SH, Hardwick JC, Diab RM, van Santen MM, Versteeg HH, van Deventer SJ, Richel DJ and Peppelenbosch MP: Activation of the canonical beta-Catenin pathway by histamine. J Biol Chem 278: 52491-52496, 2003.
17. Sastre-Perona A and Santisteban P: Role of the Wnt pathway in thyroid cancer. Front Endocrinol (Lausanne) 3: 31, 2012.
18. Gilbert-Sirieix M, Makoukji J, Kimura S, Talbot M, Caillou B, Massaad C and Massaad-Massade L: Wnt/β-Catenin signaling pathway is a direct enhancer of thyroid transcription factor-1 in human papillary thyroid carcinoma cells. PLoS One 6: e22280, 2011.
19. Veeragoni D, Ghosh H, Ansari A, Bhattacharyya S, Azaz A, Ommi O, Covarrubias-Zambrano O, Köhler LHF, Ködel JF, Hamza A, *et al*: Novel N-chloroacetyl-2-pyrazoline analogs with 2-naphthyl and ferrocenyl groups: targeting histamine receptor H1 to overcome colorectal cancer drug resistance. Cancer Drug Resist 9: 15, 2026.
20. Zhang W, Ruan X, Li Y, Zhi J, Hu L, Hou X, Shi X, Wang X, Wang J, Ma W, *et al*: KDM1A promotes thyroid cancer progression and maintains stemness through the Wnt/β-catenin signaling pathway. Theranostics 12: 1500-1517, 2022.
21. Diaz D, Bergdorf K, Loberg MA, Phifer CJ, Xu GJ, Sheng Q, Chen SC, Byrant JM, Tigue ML, Hartmann H, *et al*: Wnt/β-catenin signaling is a therapeutic target in anaplastic thyroid carcinoma. Endocrine 86: 114-118, 2024.
22. Xu Q, Yang H, Fan G, Zhang B, Yu J, Zhang Z and Jia G: Clinical importance of PLA2R1 and RASSF9 in thyroid cancer and their inhibitory roles on the Wnt/β-catenin pathway and thyroid cancer cell malignant behaviors. Pathol Res Pract 238: 154092, 2022.
23. Xu Y, Pi J, Jinghu Y, Wang X, Xu D and Liu J: Diagnostic efficiency of ACR-TIRADS score for differentiating benign and malignant thyroid nodules of various pathological types. Med Sci Monit 30: e943228, 2024.
24. Zhao Z, Ren T, Zhao Y, Xu W, Xie R, Lin J, Li H, Zheng L, Zhang C, Huo H, *et al*: Salivary biomarkers-assisted ultrasound-based differentiation of malignant and benign thyroid nodules. Gland Surg 11: 196-206, 2022.
25. Conzo G, Avenia N, Bellastella G, Candela G, de Bellis A, Esposito K, Pasquali D, Polistena A, Santini L and Sinisi AA: The role of surgery in the current management of differentiated thyroid cancer. Endocrine 47: 380-388, 2014.
26. Pizza F, Lucido FS, D'Antonio D, Tolone S, Gambardella C, Dell'Isola C, Docimo L and Marvaso A: Biliopancreatic limb length in one anastomosis gastric bypass: Which is the best? Obes Surg 30: 3685-3694, 2020.
27. Pizza F, D'Antonio D, Lucido FS, Tolone S, Del Genio G, Dell'Isola C, Docimo L and Gambardella C: The role of ursodeoxycholic acid (UDCA) in cholelithiasis management after one anastomosis gastric bypass (OAGB) for morbid obesity: Results of a monocentric randomized controlled trial. Obes Surg 30: 4315-4324, 2020.
28. Pizza F, D'Antonio D, Lucido FS, Gambardella C, Carbonell Asíns JA, Dell'Isola C and Tolone S: Does antrum size matter in sleeve gastrectomy? A prospective randomized study. Surg Endosc 35: 3524-3532, 2021.

Copyright © 2026 Sun et al. This work is licensed under a Creative Commons Attribution-NonCommercial-NoDerivatives 4.0 International (CC BY-NC-ND 4.0) License.